Viscosity of crystal-bearing melts and its implication for magma ascent

Francesco VETERE[*,**], Harald BEHRENS[**], Francois HOLTZ[**], Giuseppe VILARDO[†]
and Guido VENTURA[‡]

[*]*Dipartimento di Scienze Della Terra, Università della Calabria,
via P. Bucci I–87036 Arcavacata di Rende (CS), Italy*
[**]*Institut für Mineralogie, Leibniz Universität Hannover,
Callinstr. 3, D–30167 Hannover, Germany*
[†]*Istituto Nazionale di Geofisica e Vulcanologia, Osservatorio Vesuviano,
via Diocleziano, 328, 80124, Napoli, Italy*
[‡]*Istituto Nazionale di Geofisica e Vulcanologia,
via di Vigna Murata 605, I–00143 Rome Italy*

Experiments were performed at high temperature and pressure to determine the effective viscosity of a crystal-bearing andesite using the falling sphere method. Because viscosity experiments with partly crystallized samples are difficult to realize (i.e., due to high sensitivity of phase equilibria to P, T and water content), we have added zircon crystals to adjust precisely the volume fraction and the size of crystals in a magma. Using this approach, the anhydrous melt composition does not vary significantly with temperature and water content of the melt and, hence, the effects of crystals on effective viscosity can be worked out accurately. The investigated systems (magma analogue) were composed of an andesitic melt containing 0.5 wt% to 4.1 wt% H_2O and 15 vol% to 40 vol% of zircon crystals with grain size <100 μm. Most experiments were performed at 300 MPa and 1523 K. The ZrO_2 content dissolved in the melt under these conditions is 1.61 wt% ± 0.16 wt% (0.5-4.0 wt% H_2O in melt) with no significant dependence on water content, which is about twice the value predicted by the model of Watson and Harrison (1983).

The falling velocity of large platinum spheres was measured in the experimental magmas. The radius of the spheres (between 130 μm and 510 μm) was always much larger than the crystal sizes and the inter-grain distances, implying that the falling velocity of the spheres can be used to calculate the effective viscosity of the magmas. For magmas containing 15 vol% zircon, the measured viscosity was 0.7 log to 1.6 log units higher than the melt viscosity. The effective magma viscosity is higher than expected from literature models. The spheres did not move in systems containing 30 vol% to 40 vol% of crystals, even after 16 h at 1523 K. We attribute this observation to the presence of yield strength of more than 100 Pa, i.e., a threshold of accelerating force needs to be passed before the sphere can move in the magma.

Keywords: Viscosity, ZrO_2 solubility, Magma, Falling sphere method, Crystal-bearing andesite

INTRODUCTION

The most important factors governing the rheological properties of magmas are the viscosity of the liquid phase and the fraction of crystals. The melt viscosity depends strongly on temperature and melt composition including the amount of dissolved volatiles, in particular dissolved water (see recent models of Hui and Zhang, 2007; Giordano et al., 2008; and references therein). On the other

hand pressure has usually only minor influence on viscous flow at crustal pressures (e.g., Scarfe et al., 1987; Behrens and Schulze, 2003). Often the effective viscosity of melts containing nearly spherical crystals is estimated with the Einstein-Roscoe equation (Einstein, 1906; Roscoe, 1952):

$$\eta_{eff} = \eta_m (1 - \phi/\omega)^{-2.5} \qquad (1),$$

where η_{eff} is the effective viscosity of the liquid with a volume fraction ϕ of crystals, and η_m is the viscosity of the melt. The parameter ω corresponds to the crystal fraction

at which a transition of the system to the rigid state occurs. According to Marsh (1981) a value of 0.6 for ω is suitable to estimate the effect of crystals on the relative viscosity (η_{eff}/η_m) in magmatic systems. Experimental data for partially crystallized $Mg_3Al_2Si_3O_{12}$ and $Li_2Si_2O_5$ systems containing spherical crystals confirm the validity of Einstein-Roscoe equation with $\omega = 0.6$ for systems containing up to 40 vol% and 30 vol%, respectively, in the region of high melt viscosities (Lejeune and Richet, 1995). More complex relationships with additional adjustable parameters are required to describe the variation of the relative viscosity in the full range from the pure melt to the completely crystallized system (Sherman, 1968; Costa, 2005; Rosenberg and Handy, 2005).

In crystal-bearing melts it is not only the fraction of crystals which is important but also the shape and the size of the crystals (e.g., Kerr and Lister, 1991; Pinkerton and Stevenson, 1992; Arbaret et al., 2007). Simha (1940) derived a theoretical equation that describes the effect of the non-sphericity of crystals on the relative viscosity of crystal suspensions and gave approximate equations for large axial ratios. For thin disks, the multiplier for the relative viscosity η_r to account for the axial ratio f is $16f/15 \tan^{-1}f$. Another complexity of magmas is that ϕ changes progressively during magma differentiation and the composition of residual liquid changes as well (Getson and Whittington, 2007). This makes it extremely difficult to study experimentally the change of the effective viscosity of a magma as a function of temperature and volatile content.

Sato (2005) analyzed viscosity variations of dry high-Al basalt from the Fuji volcano (Japan) in the temperature range 1503–1403 K. The results show an increase in viscosity from ~ 52 Pa·s at 1503 K (above the liquidus) to ~ 1950 Pa·s at 1403 K when the crystal content reached 23 vol%. In the study of Sato (2005), the observed increase in viscosity was related to the increase of the crystal fraction and the concomitant increase of the SiO_2 content in the melt due to crystallization. The effective viscosity is larger by a factor of 4–5 with respect to the predictions of Eq.(1). In the viscosity calculation, Sato (2005) has estimated the melt viscosity along the differentiation path using the model of Shaw (1972). The equation derived from this study allows calculating the effective viscosity of partially crystallized basaltic magma from Fuji volcano as follow:

$$\eta_{eff}/\eta_m = 0.832 \cdot exp(13.06 \cdot \phi) \qquad (2).$$

Sato (2005) suggested that the difference to the predictions of Simha (1940) might be due to variations in crystal sizes and alignment (mainly plagioclase with an average aspect ratio of 12.9) of the crystals during experiments

using the rotational cylinder method.

Another difficulty in experimental studies on rheological properties of crystal-bearing melts and in the application of the data is the deviation from Newtonian behavior of the magma (the effective viscosity may become dependent on the applied forces). Using torsion experiments with haplogranite melts containing 2.5 wt% H_2O and various amounts of corundum crystals, Arbaret et al., (2007) showed that, at 300 MPa confining pressure and at temperatures between 748 K and 1273 K, the flow is Newtonian only for $\phi \leq 0.16$. At higher volume fractions of crystals, the melt-crystal system behaves increasingly Non-Newtonian with an increase in apparent viscosity by more than one order of magnitude from $\phi = 0.16$ to $\phi = 0.54$ at a strain rate of $6 \cdot 10^{-4}$ s^{-1}. Champallier et al., (2008) investigated the rheological behavior of synthetic crystal-bearing haplogranitic magma (~ 2.5 wt% water in the melt) containing up to 76 vol% of Al_2O_3 crystals at a confining pressure of 300 MPa and temperatures between 748 K and 1273 K at shear rates between 10^{-4} and 2 × 10^{-3} s^{-1}. Shear viscosity measurements were performed in torsion (simple shear). For pure hydrated melt and for 16 vol% of crystals, the rheology is found to be Newtonian. The Einstein-Roscoe equation adequately estimates viscosities of the crystal-bearing magmas at low crystal contents ($\phi \leq \sim 0.25$), but progressively deviates from the measured viscosities with increasing crystal content as the rheological behaviour becomes non-Newtonian. At higher crystal contents, the magmas exhibit shear thinning behavior (pseudoplastic). Shear-thinning behavior was also observed by Ishibashi (2009) in a basaltic melt containing plagioclase (experiments performed at 1470 K with basalt from Fuji volcano).

Caricchi et al., (2007) performed creep experiments on haplogranitic melts containing 2.7 wt% of dissolved water and various amounts of quartz crystals using a Paterson apparatus. In the temperature range 773–1173 K and at 250 MPa confining pressure, they observed a Newtonian behavior of the system only for strain rates less than 10^{-5} s^{-1}, independent on the volume fraction of crystals. Above this threshold, an increase of strain rate always induced a decrease of viscosity (shear thinning). A shear-rate dependence of viscosity was noticed as well by Sato (2005) for partially crystallized basalt with high fractions of crystals (low temperature) using rotational viscometry at ambient pressure.

Experimental investigations on the rheology of crystal-bearing natural melts focused on either granitic or basaltic systems. Data for intermediate compositions such as andesite are missing. Here, we present a novel experimental technique to study the rheological properties of crystal-bearing melts based on the falling sphere method. Us-

ing large platinum spheres the effective viscosity of the crystal + melt system can be measured. Furthermore, these experiments may yield information on the behavior of large sinking crystals in magma chambers. We have tested this technique on crystal-bearing andesites at temperatures relevant for magmatic processes (1373-1523 K). The variation of crystal contents was achieved by adding zircon crystals to the andesitic melt at temperatures above the liquidus (liquidus conditions would be reached if the melts would be undersaturated with respect to zircon). While doing so, we avoid complexities in the interpretation of the experimental results because the melt composition does not change as a result of changing temperature and partial crystallization. Considering that the zircon solubility does not change significantly, the melt composition remains basically unchanged upon variation of temperature.

EXPERIMENTAL AND ANALYTICAL METHODS

The starting material was a synthetic basaltic-andesite with composition close to Unzen Volcano (Pre Unzen 500 kyr; Chen et al., 1993) (MDIB, Table 1). About 100 g of glass was produced by melting a mixture of oxides and carbonates at 1873 K for 4 h in a Pt crucible in air. The melt was quenched by pouring on a brass plate. To improve homogeneity, the glass was crushed, re-melted and quenched at same conditions. The composition of the obtained glass measured by electron microprobe analyses (EMPA) is given in Table 1.

In the next step we have synthesized hydrous glasses at high pressure as described in Vetere et al., (2008). All the high pressure and high temperature experiments were performed at the Institute of Mineralogy (Leibniz University of Hanover). Between 1 wt% and 4 wt% of distilled

water was added stepwise to a dry glass powder in AuPd capsules (inner diameter of 5-6 mm, length of 30-40 mm). Additionally, we filled one capsule with glass powder without adding water in order to equilibrate the glass at the experimental conditions (300 MPa) used to measure viscosities. After welding shut, capsules were processed in an internally heated gas pressure vessel (IHPV) at 300 MPa and 1523 K over night. Redox conditions are close to the $MnO-Mn_3O_4$ buffer when a pure H_2O fluid is present in the capsule (Berndt et al., 2002). In our syntheses the melts were always water-undersaturated and, hence, the oxygen fugacity was lower. Samples were rapidly quenched after the experiment (see Berndt et al., 2002), resulting in crystal-free and bubble-free glasses. The water contents of the glasses were determined after thermal decomposition using Karl-Fischer titration (Behrens, 1995). An increment of 0.10 wt% was added to the measured values to account for unextracted water in the glasses after analyses (Leschik et al., 2004). It is noteworthy that the nominally anhydrous sample (no water was added) also contained significant water after synthesis (up to 0.52 wt%, Table 2). This is due to diffusion of hydrogen from the pressure medium into the capsule and subsequent reaction with ferric iron ($Fe_2O_3 + H_2 = 2 FeO + H_2O$). The redox state of iron was not determined for the glasses but is expected to be similar to that of andesitic glasses with similar water contents (Vetere et al., 2008).

The powder of glasses (grain size fraction between 100 μm and 250 μm) was manually mixed with zircon powder of well-defined grain size and loaded into AuPd capsules (inner diameter of 6 mm, length 30-40 mm). Zircon crystals were purchased from the company Dr. F. Krantz, Rheinisches Mineralien-Kontor GmbH & Co. Bonn, Germany (zircon concentrate # X03714, Australia). The selected crystals (1 mm to 1 cm in diameter) were crushed and sieved using a mesh of 100 μm in diameter. The obtained zircon powder was shaken for some minutes in a glass beaker filled with deionized water and then the liquid was decanted to remove fine crystals.

The size of the zircon particles ranges from 0.6 to 59 μm with a mean of 4.9 μm (determined using image analysis). Glass-zircon mixtures were compacted with a steal piston before welding shut. Then the capsules were processed in the IHPV for 180 min at 300 MPa and 1523 K except for one experiment at lower temperature (Zr1, 1473 K). After rapid quench, the synthesis products contain no other phases than zircon and glass. The compositions of two zircon crystals measured by EMPA are listed in Table 1. No other elements than Zr and Si were detected in significant concentrations. However, the difference of the totals to 100 wt% may indicate the presence of other elements which were not analyzed by EMPA (such as

Table 1. Electron microprobe analyses of the starting glass and two selected zircon crystals (wt%)

	Andesite MDIB	STD	Zr_core1	STD	Zr_core2	STD
SiO_2	54.18	(0.60)	32.18	(0.19)	32.16	(0.38)
TiO_2	1.09	(0.07)	0.02	(0.00)	0.02	(0.01)
Al_2O_3	18.41	(0.19)	0.02	(0.00)	0.01	(0.01)
$^§FeO$	9.52	(0.33)	0.13	(0.09)	0.15	(0.04)
MnO	0.09	(0.06)	0.11	(0.10)	0.07	(0.06)
MgO	2.93	(0.09)	0.05	(0.00)	0.02	(0.02)
CaO	8.69	(0.32)	0.05	(0.00)	0.04	(0.02)
Na_2O	3.41	(0.29)	b.l.d.	(-)	b.l.d.	(-)
K_2O	1.42	(0.08)	0.02	(0.01)	0.02	(0.01)
ZrO_2			65.82	(0.48)	65.98	(0.29)
Total	100.02		98.29		98.41	

§ Total iron is given as FeO.
1 σ standard deviation is given in parentheses.

Table 2. Composition of glasses after equilibration with zircon normalized to 100 wt%

	Zr1		Zr2		Zr4		Zr7		Zr13A		Zr20A	
SiO_2	50.33	(0.41)	51.82	(0.55)	52.83	(0.47)	53.77	(0.41)	54.45	(0.59)	52.38	(0.51)
TiO_2	1.11	(0.05)	1.03	(0.05)	1.06	(0.06)	1.09	(0.07)	1.09	(0.09)	1.05	(0.04)
Al_2O_3	18.38	(0.31)	17.94	(0.20)	17.86	(0.30)	18.43	(0.27)	17.93	(0.21)	17.48	(0.15)
$^§FeO$	8.89	(0.38)	8.45	(0.38)	8.35	(0.44)	8.46	(0.58)	8.9	(0.48)	8.21	(0.31)
MnO	0.00	(0.07)	0.03	(0.07)	0.01	(0.07)	0.01	(0.07)	0	(0.07)	0.06	(0.07)
MgO	3.44	(0.12)	3.32	(0.13)	3.26	(0.12)	3.41	(0.11)	2.77	(0.08)	2.69	(0.12)
CaO	7.94	(0.15)	7.79	(0.24)	7.65	(0.22)	8.00	(0.21)	8.18	(0.26)	7.96	(0.14)
Na_2O	3.24	(0.19)	3.13	(0.19)	3.1	(0.18)	3.24	(0.19)	3.26	(0.23)	3.00	(0.15)
K_2O	1.48	(0.07)	1.49	(0.08)	1.47	(0.08)	1.59	(0.09)	1.45	(0.08)	1.34	(0.06)
ZrO_2	1.67	(0.08)	0.92	(0.18)	1.45	(0.17)	1.48	(0.20)	1.47	(0.14)	1.83	(0.14)
$^\#H_2Otot$	3.52		4.07		2.96		0.53		0.50		4.00	
Vol% zircon added	9		15		15		15		15		15	

	Zr21A		Zr13B		Zr20B		Zr21B		Zr40	
SiO_2	53.32	(0.35)	54.44	(0.34)	52.19	(0.37)	53.55	(0.20)	55.51	(0.79)
TiO_2	1.09	(0.07)	1.10	(0.07)	1.04	(0.06)	1.09	(0.05)	1.09	(0.08)
Al_2O_3	18.11	(0.04)	18.25	(0.27)	17.38	(0.08)	17.81	(0.44)	18.57	(0.56)
$^§FeO$	8.31	(0.19)	8.44	(0.48)	8.50	(0.39)	8.37	(0.43)	6.65	(0.35)
MnO	0.03	(0.02)	0.01	(0.09)	0.09	(0.08)	0.03	(0.07)	0.03	(0.10)
MgO	2.77	(0.15)	2.77	(0.11)	2.70	(0.04)	2.75	(0.10)	2.79	(0.12)
CaO	7.88	(0.19)	8.20	(0.21)	8.03	(0.16)	8.16	(0.16)	8.39	(0.33)
Na_2O	3.03	(0.13)	3.09	(0.16)	3.04	(0.18)	3.17	(0.21)	3.26	(0.21)
K_2O	1.44	(0.11)	1.46	(0.06)	1.39	(0.05)	1.43	(0.05)	1.47	(0.06)
ZrO_2	2.04	(0.14)	1.73	(0.18)	1.65	(0.33)	1.7	(0.08)	1.74	(0.12)
$^\#H_2Otot$	1.97		0.50		3.99		1.94		0.50	
Vol% zircon added	15		30		30		30		40	

All samples were synthesized for 180 min at 1523 K and 300 MPa except for Zr1 which was processed for 210 min at 11473 K, 300 MPa.

1 σ standard deviation is given in parentheses.

refers to the water content of the pre-hydrated glasses measured by KFT.

§ Total iron is given as FeO.

Hf and REE which are common elements in zircons). The compositions of glasses after reaction with zircon are reported in Table 2. No significant difference to the starting glasses was observed except for the ZrO_2 content when taking into account the water content.

The zircon-bearing glass bodies had almost cylindrical shape. For the viscosity experiments we cut two cylinders with length of ~ 2 mm and ~ 15 mm perpendicular to the axes. The rest of the sample was crushed. The capsules for viscosity determination were prepared with the following steps:
1) Part of the crushed material was placed in the bottom of a AuPd capsule (6 mm diameter).
2) The short cylinder was inserted.
3) A small portion of Pt powder with 1 μm grain size was loaded on top of this cylinder to be used as internal reference for distance measurements.
4) The 15 mm long cylinder was inserted.
5) The rest of the crushed material was loaded on the top.
6) A Pt sphere with radius between 130 and 510 μm was pressed into the centre of the powder until it was in contact with the long cylinder.

After welding shut the capsule, a pre-viscosity experiment was performed in an IHPV at 1523 K and 300 MPa for a few minutes to establish well-defined starting positions of the spheres with respect to the Pt powder layer. After measuring the sphere position using X-ray images, falling sphere experiments were performed at 1373–1523 K at a confining pressure of 300 MPa. Run duration varied between 10 min and 1000 min. All experiments were finished by rapid quench.

X-ray images were used to monitor the sphere positions in the quenched samples (de Götzen xgenus® dc camera with digital scanning image, exposure time of 0.20 s in Rome; Misiti et al., 2006). The large Pt spheres could be identified easily in the X-ray radiographs without removing the AuPd capsule. Two images with different orientations of the sample (perpendicular to each other) allowed us to measure the positions of the sphere relative to the Pt marker and relative to the capsule walls. The settling distance of the sphere could be measured (with an error of ±20 μm) by superimposing images collected be-

fore and after experiments. The viscosity η is calculated by Stokes law:

$$\eta = \frac{2 \cdot t \cdot g \cdot \Delta\rho \cdot r^2 \cdot C_F}{9 \cdot d} \qquad (3),$$

where d is the settling distance in m, t is the run duration in sec, $\Delta\rho$ is the density difference between the sphere and the melt (calculated after Vetere et al., 2008), g is the acceleration due to gravity (9.81 m/s^2), r is the radius of the sphere. Based on a theoretical approach, Faxen (1923) derived a relationship for the effect of viscous drag by the capsule wall on the settling sphere C_F where R is the inner radius of the capsule:

$$C_F = 1 - 2.104\left(\frac{r}{R}\right) + 2.09\left(\frac{r}{R}\right)^3 - 0.95\left(\frac{r}{R}\right)^5 \qquad (4).$$

Although there might be some uncertainty in the validity of the Faxen correction (Kahle et al., 2003), we applied Eq. (4) to all our experiments for internal consistency and for consistency with previous studies. To account for movement of spheres during heating and cooling, we calculated the effective run duration for each experiment as described in Vetere et al., (2006). Since we do not know the activation energy for viscous flow of the crystal-bearing melts, we have used the data for the pure melts to estimate the time increment for heating and cooling. In the calculation we have used the room temperature density of Pt of 21.45 g/cm^3. No correction was made for differential compression and thermal expansion of the sphere because this would contribute less than 1% to the viscosity value. The sphere radius was measured before the experiments. Within the resolution of the X-ray images we could not see any changes in sphere shape after pressurization.

RESULTS AND DISCUSSION

Zr content of the glasses

Figure 1 shows back scattered electron images of three samples produced by reaction of 15 vol%, 30 vol% and 40 vol% added zircon with andesitic melts. The shape of the zircon crystals do not show any dissolution features, i.e., sharp edges are still preserved. Fine grained zircons are almost absent in most of the images and we conclude that such small crystals probably dissolved preferentially to saturate the melt with respect to ZrO_2. The concentration of ZrO_2 in glasses produced at 1523 K varies between 1.43 wt% and 2.04 wt% with no systematic dependence on volume fraction of added zircon (Fig. 2 and Table 2). At 1523 K, the glasses containing ~ 0.5 wt% H_2O have
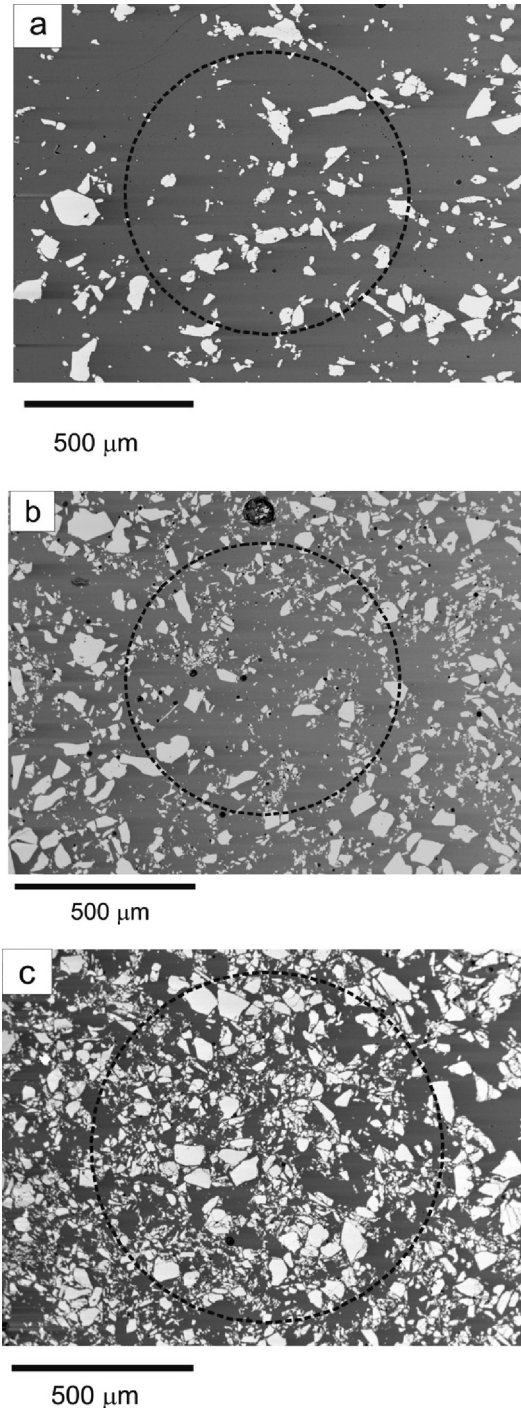

Figure 1. Backscattered electron image of zircon-bearing andesitic glasses after equilibration with zircon crystals at 1523 K, 300 MPa (a) with 15 vol% added zircon (Zr2), (b) with 30 vol% added zircon (Zr21B) and (c) with 40 vol% added zircon (Zr40). Dashed circles represent the size of the spheres utilized in the viscosity experiments.

slightly lower ZrO_2 concentrations than those containing higher H_2O concentrations (Table 3). The run duration was not varied to check for equilibrium between zircon and melt. However, the evolution of ZrO_2 concentrations
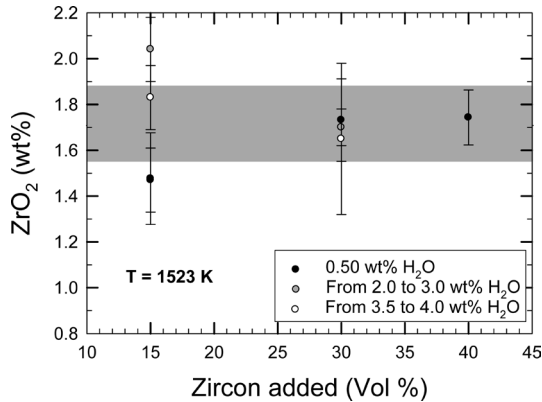
Figure 2. ZrO_2 contents of andesitic glasses after equilibration of melts with zircon at 1523 K. The dashed line represents the average value, the grey box signifies the 90% confidence interval (wt%) of the analysis of ZrO_2 concentrations.

in glasses obtained from experiments with different volume fraction of zircon is useful to test equilibrium conditions because the inter-grain distance decreases strongly from 15 vol% to 40 vol% zircon (Fig. 1). At a given temperature and melt water content, the variations are within analytical error (compare data for 0.5 wt% H_2O in melt), indicating that the measured concentrations are close to the equilibrium values.

Watson and Harrison (1983) determined experimentally the solubility of zircon in aluminosilicate melts (granitic to andesitic melts) as a function of both temperature and composition. Based on the experimental data a model for the prediction of zircon solubility was proposed:

$$\ln D_{Zr} zircon/melt = -3.80 - \left[0.85 \cdot (M-1)\right] + \frac{12900}{T} \quad (5),$$

where D_{Zr} zircon/melt is the concentration ratio of Zr (in wt%) in the stoichiometric zircon to that in the melt, T is the absolute temperature, and M is the cation ratio (Na + K + 2Ca)/(Al·Si). This model mainly bases on experiments with water-rich melts at 1133 K, 1203 K and 1293 K, but has been also confirmed at temperatures up to 1773 K for $M = 1.3$ (peraluminous granite). According to Eq. (5) a ZrO_2 concentration of 0.87 wt% is expected at 1523 K for the andesitic melt (with M = 1.378). The experimental ZrO_2 content of the melt is roughly twice this value. The difference might be due to missing experimental data for andesite melts at high temperature in the calibration of the model.

Image analyses of zircon-bearing glasses

According to Simha (1940) and Kerr and Lister (1991), the shape of crystals has strong influence on the viscosity

of crystal-bearing systems. For example, for a given volume fraction of solid material, the viscosity of a suspension will increase when the particles become elongated because the drag exerted by a particle is proportional to its longest dimension. The shape (angular vs. rounded particle) may also influence the viscosity. However, it is still poorly known how the mineral shape affects quantitatively the effective viscosity of a crystal mush. The viscosity should increase if the particles have more irregular shape because the irregularity of the particles exerts a 'resistance' in the flow of the suspension. Taking these observations into account, we conducted an image analysis of the zircon crystals to check if the crystals have the same shape features in the different experimental runs. If not, the measured viscosities cannot be directly compared and the effects of the shape on the viscosity should be taken into account.

BSE images from each synthesized zircon-bearing andesite glass were analyzed to get information about the volume fraction and the shape distribution of crystals. Figure 1 shows a good homogeneity of the "magma" on a millimeter scale. Image analysis was performed to extract and characterize the crystal shapes from the input gray-scale slides. In order to identify the particle to be analyzed, it was necessary to transform the original 256 grey level images (Fig. 3, left) into binary ones (Fig. 3, center) (Dellino and La Volpe, 1996; Loncaric, 1998). To ensure a precise thresholding of the resulting binary objects, we performed the following steps. We inspect the pixel histogram that represents the number of pixel for each grey level of the image and select the light gray-scale range corresponding to the intensity of the particle and assign to all other pixel the background value zero. First, white color and pixel value 1 was assigned to the whole selected gray-scale range approximately corresponding to the crystal areas, then a thresholding operation was performed in order to highlight the particle outline and separate boundaries of particles next to each other. The remaining classes were merged to the background by assigning to the pixels the value 0 (Fig. 3, center). On the binary images obtained from the whole dataset of input gray-scale slides, the ArcInfo software (ESRI) was used to identify each crystal. The software recognizes as a particle each group of adjacent pixels which have a value equal to 1 contoured in all direction by pixels having a level 0 (Fig. 3, right). Finally, for each recognized two-dimensional object, the program calculates the following shape parameters: area, perimeter, the centroid coordinates, the lengths of the major and minor axes and the orientation of the major axis. Following Cox and Budhu (2008), the following two shape parameters were determined for each particle:
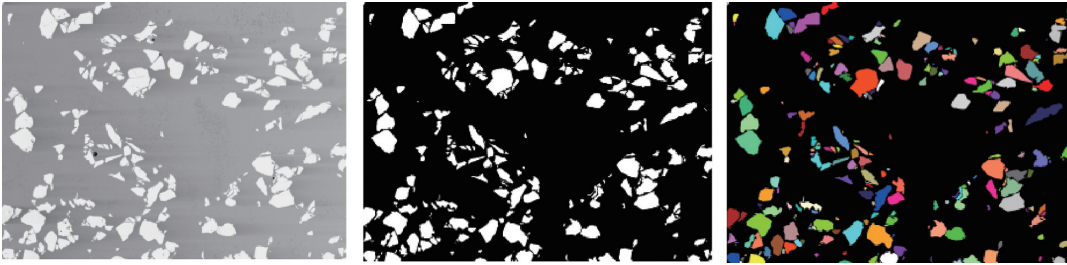
Figure 3. Experimental sample Zr2: original grey tones BSE image (left); processed binary image, black, matrix; white, crystals (center); color coded image in which different colors represent distinct recognized objects (right).
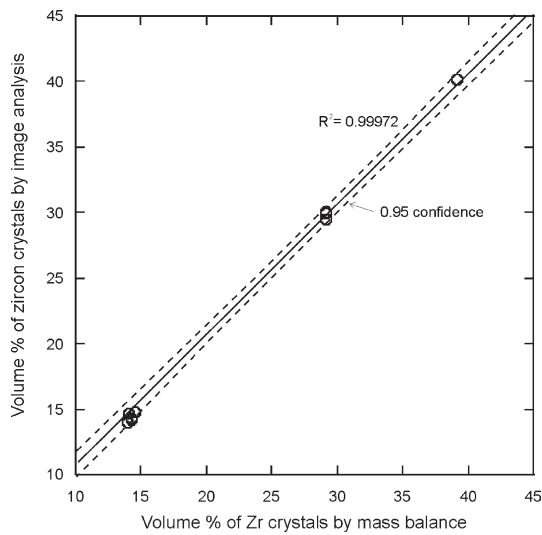

Figure 4. Comparison between the volume percentages of zircon crystals in andesitic glasses determined by mass balance (Table 3) and by image analysis of BSE images.

aspect (AS) = *major axis/minor axis*

form factor (FF) = $(4\,\pi\,surface)/(perimeter^2)$.

AS and FF give information on the particle elongation and the surface irregularities (roughness), respectively. A circle, which represents a perfectly rounded particle, has FF = 1. As the irregularity of the particle shape increases, FF decreases. The counted crystals in each analyzed image (one or two images of 1500 × 1100 μm for each sample with a resolution of 1200 dpi) vary from 270 to 2640. Using the measured ZrO_2 concentrations in the glasses, the initially added volume fractions of zircon, and the density of the phases, [zircon 4650 kg/m^3, Deer et al. (1992); andesite glass: $(2661-8.4\cdot wt\%\ H_2O)$ kg/m^3, Vetere et al. (2008)] we calculated the volume fractions of zircons present during viscosity experiments (Table 3). The good agreement between volume fractions of zircon derived by mass balance and by image analyses (Fig. 4)
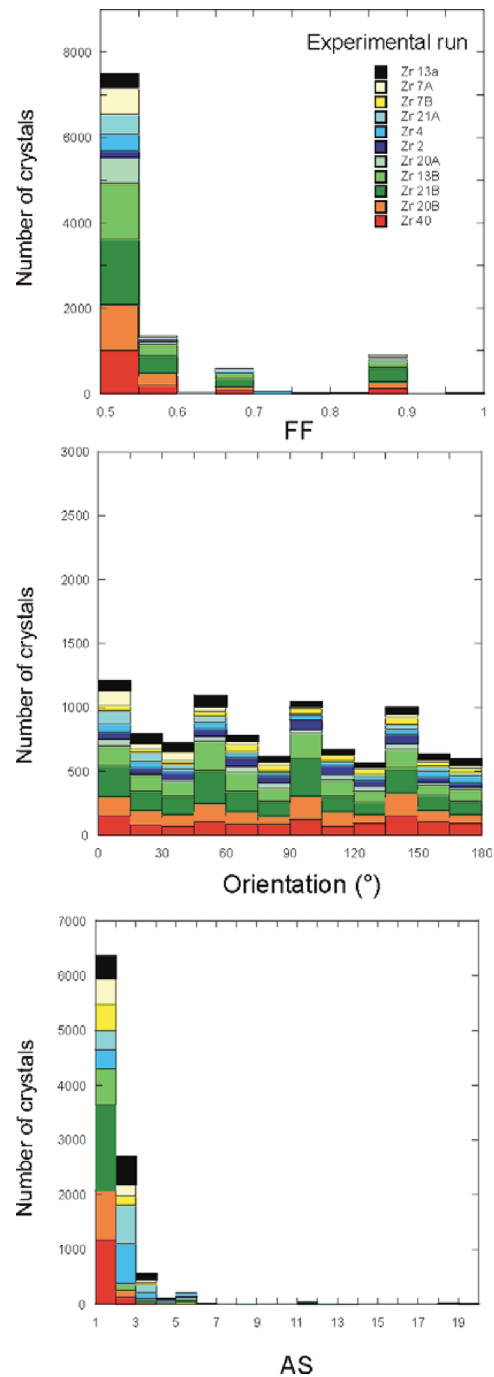

Figure 5. Distribution of size, shape parameter FF, orientation, and aspect ratio AS of zircon crystals in the experimental products. Data are based on one or two BSE images.

confirmed the accuracy of thresholding used in images analyses. Differences between the volume percent determined by mass balance and image analysis are within 0.95 confidence and vary from 0.03 vol% to 0.97 vol%.

Figure 5 summarizes the distributions of the shape parameters of the zircon crystals in the different experimental runs. The distributions of FF, AS and crystal orientation are very similar in the different experimental runs. The calculated FF values indicate an angular shape of the zircon particles similarly as observed for magmatic rocks (e.g., Iezzi and Ventura, 2002). Also, the crystals do not show a clear preferred orientation, i.e. no alignment. The majority of the particles are only slightly elongated with 92 % of particles having AS ≤ 3 and 65 % with AS ≤ 2. The shape distributions of the zircon crystals in the different experimental runs are comparable and the viscosities measured in the different runs are comparable as well. On the basis of the image analysis data, possible effects of variations of crystal shapes and/or orientation on viscosity measurements are the same for all the experiments. In addition, the relationship between the viscosity of the melt plus crystals suspension and the crystal shape is given by (Mandal et al., 2000):

$$\eta_{eff} = \{1 + [2\phi/ab^2(a^2 + b^2)]1/\beta\}\eta_m \qquad (6),$$

where φ is the crystal fraction, a is the major axis of crystal, b is the minor axis and β is a shape factor. If crystals have $a–b$ (i.e., AS ~ 1, as shown in Fig. 5), $\beta = 2a^{-5}/5$, and equation 5 reduces to the Einstein–Roscoe relation (Man-

dal et al., 2000). Therefore, the crystal population of zircon in our experiments may be approximated to a population of spheres and possible effects of the shape on viscosity are not relevant.

Falling sphere experiments

In total eleven falling sphere experiments were performed in model magmas formed of melts containing 0.5 wt% to 4.1 wt% H_2O and 14.0 vol% to 39.1 vol% zircon crystals (Tables 2 and 3). A descent of the sphere was observed only in six of the experiments with 15 vol% of zircon added. At 1523 K , a measurable movement of the sphere was not observed in runs with 30 vol% zircons (Zr13B, Zr20B and Zr21B) and 40 vol% zircon (Zr40) although run durations were much longer than in the other experiments. Thus, there appears to be a threshold between 15 vol% and 30 vol% of crystals where the force induced by the sphere becomes insufficient for acceleration of the sphere. As shown in Figure 1 the distance between the crystals is already extremely small at 30 vol% crystal content so that they can migrate only by cooperative processes which need larger forces.

In one experiment with 15 vol% added zircons (Zr21A), the sphere did not move significantly although a noticeable displacement would be expected from the comparison with the whole experimental dataset (experiments with 15 vol% added zircons). One possible reason is that the sphere was too close to the capsule wall, as recorded via X-ray images (leading to a Faxen correction

Table 3. Experimental conditions and results of viscosity experiments

No.	Zircon By mass balance (vol%)	ZrO$_2$ In the glass (wt%)	H$_2$O In the glass (wt%)	T (K)	Sphere radius (μm)	C$_F$	Dwell time (s)	Corrected time (s)	Falling distance (cm)	Log η This work (Pa·s)	Log η Melt$^\$$ (Pa·s)	Log η Einstein-Roscoe model (Pa·s)	Log η Sato (2005) model (Pa·s)
Zr13A	14.26	1.47	0.50^t	1523	280 ± 5	0.81	5920	5993	1.204	3.11	2.65	2.94	3.38
Zr7a	14.28	1.43	0.52^t	1523	465 ± 5	0.83	1800	1849	0.721	3.28	2.64	2.93	3.37
Zr7b	14.28	1.43	0.52^b	1523	465 ± 5	0.83	3600	3649	1.072	3.40	2.64	2.93	3.37
Zr21A	13.97	2.04	1.98^t	1523	330 ± 5	0.77	900	973	-	-	1.86	2.14	2.57
Zr4	14.26	1.45	2.98^b	1423	420 ± 5	0.85	600	643	0.388	3.01	1.91	2.21	2.64
Zr2	14.53	0.92	4.02^b	1373	420 ± 5	0.85	600	640	0.248	3.20	1.83	2.13	2.57
Zr20A	14.06	1.83	4.08^t	1523	130 ± 5	0.91	900	973	1.137	1.75	1.15	1.44	1.87
Zr13B	29.13	1.74	0.50^b	1523	510 ± 5	0.65	57610	57696	-	-	2.65	3.37	4.22
Zr21B	29.14	1.70	1.98^c	1523	380 ± 5	0.74	3660	3797	-	-	1.86	2.58	3.43
Zr20B	29.15	1.65	4.08^c	1523	260 ± 5	0.82	1800	1937	-	-	1.15	1.88	2.73
Zr40	39.13	1.74	0.50^c	1523	420 ± 5	0.71	59340	59513	-	-	2.65	3.80	4.79

In experiment Zr7b the sample from Zr7a was used.

Spheres radii were determined before the experiment. C$_F$ refers to the Faxen correction. Supscripts t, b and c at water contents refer to KFT analyses of pieces from the top, the bottom and the center of the prehydrated glass bodies, respectively.

Vol% zircon was calculated by mass balance using the measured ZrO$_2$ content of the glasses and the added amount of zircon.

$^\$$ calculated melt viscosity after Vetere et al. (2008) for Fe^{2+}/Fe$_{tot}$ = 0.70.

$C_F = 0.56$ Table 3), so that the drag effects may have prevented any movement. Three experiments Zr7a, Zr7b and Zr13A (all with a crystals content of 15 vol% and a water content of ~ 0.5 wt%) were performed at 1523 K with durations of 1849 s, 3649 s and 5993 s, respectively (Table 3). The viscosities derived from these experiments yield an average value of $10^{3.26}$ Pa·s. The effective viscosities differ by less than 0.3 log units and show no correlation to run duration.

The time-independence of effective viscosity suggests that stable conditions of the crystal-melt system are established already after the pre-experiments. This statement is supported by estimates of the falling distance of free zircon crystals in the melt. According to Eq. (3) the largest crystals with radii in the order of 60 μm (Fig. 1) will sink by 0.1-0.4 mm during experiments Zr7a, Zr7b and Zr13A, which is much longer than the inter-grain distance.

At the same temperature (1523 K), sample Zr20A with 4.08 wt% H_2O dissolved in the melt yielded an effective viscosity of $10^{1.75}$ Pa·s which is about 1.5 log unit lower than for the water-poor melts (Table 3 and Fig 6). When comparing the effective viscosities of zircon-bearing andesites (15 vol%) with pure andesitic melts at 1523 K, it can be noted that the melt viscosities are lower by ~ 0.8 log units. This difference in viscosity is the same for melts containing ~ 0.5 wt% and 4.1 wt% H_2O.

Two experiments with melts containing ~ 4.0 wt% H_2O performed at 1523 K and 1373 K, respectively, allow us to discuss the effect of temperature on the effective viscosity. The effective viscosity of zircon-bearing melts increases by 1.5 log unit when the temperature decreases from 1523 K to 1373 K (Zr20A and Zr2, Table 3) while the viscosity of the crystal-free melt only increases by 0.7 log unit at same conditions (Fig. 6). The relative viscosity η_r ($\eta_r = \eta_{eff}/\eta_m$) at 1523 K is ~ 4 whereas it is 23 at 1373 K. Such a variation is not expected and the low temperature value seems to differ from the η_r of all other experiments (variation from 2.9 to 5.7 at 1523 K). One explanation may be that the temperature of the experiment at 1373 K was below the liquidus. The liquidus curve for an andesite melt (Table 1) is shown in Figure 7 for a water content covering all the experimental dataset (calculation using PELE software for pressure of 300 MPa, Boudreau, 1999). Following this model, all the experiments have been performed at supraliquidus conditions except the experiment performed at 1373 K. However, a comparison with phase equilibria experiments in andesitic melt with a slightly different composition show that supraliquidus conditions should be reached at ~ 1330 K for 4 wt% water in the melt (Botcharnikov et al., 2008). Using microprobe, we did not observe the presence of new phases. Thus, the
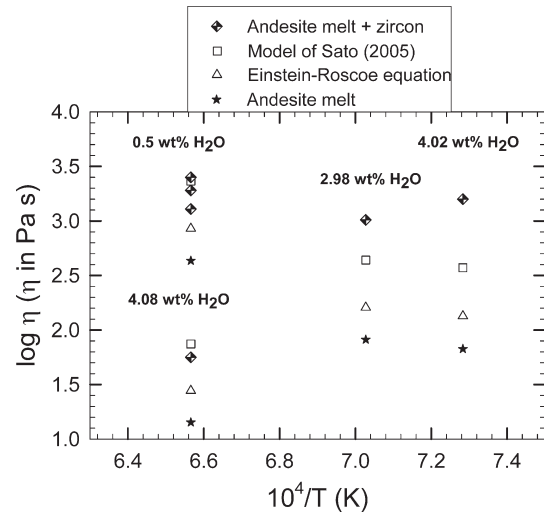

Figure 6. Comparison of the effective viscosities of crystal-bearing andesite with the viscosity of the crystal-free melts calculated after Vetere et al. (2008), and with predictions by the Einstein-Roscoe equation and the model of Sato (2005).
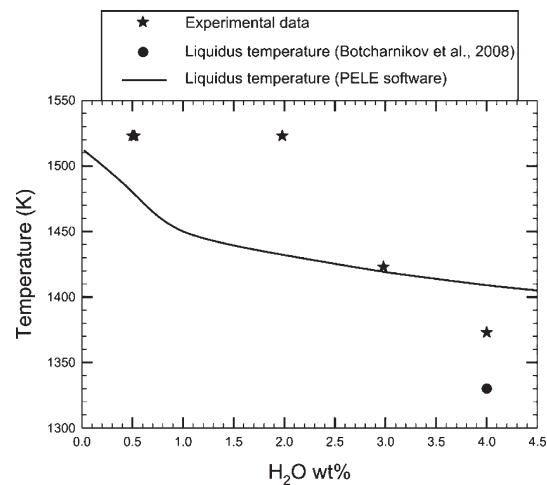

Figure 7. Liquidus temperature of the andesitic melt used in this study as a function of H_2O content, calculated at 300 MPa showing using the PELE software (solid line, Boudreau, 1999). Black stars represent the experimental temperature. Note that the liquidus temperature for a slightly different andesitic composition (but more Mg-rich than the composition used in this study) containing 4 wt% water is ~ 1330 K (see black circle in Fig. 7; Botcharnikov et al., 2008).

larger value of η_r at 1373 K can not be explained by the partial crystallization of the andesitic melt. In fact, the variation between the η_r at 1373 K and η_r observed at higher temperatures can be explained if the error on the determination of η_m and the error derived from the falling sphere method is taken into account (similar value within error).

DISCUSSION

Comparison with previous models

The results of the viscosity measurements with 15 vol% added zircons are compared to the melt viscosity and to the predictions of models in Figure 6. Melt viscosity was calculated using the equation derived for the same andesite composition (Vetere et al., 2008). To account for the effect of dissolved ZrO_2, the viscosity model of Giordano et al. (2008) was applied assuming that dissolved Zr behaves as Ti. Using this model and assuming a ZrO_2 concentration of 2 wt%, the melt viscosity increases by approximately 0.3 log units at 1523 K. For comparison we have calculated the effective viscosity of the crystal-melt suspension with the Einstein-Roscoe equation using the parameter $\omega = 0.6$ from Marsh (1981) taking into account that the shape of the zircon crystals may be approximated to that of spheres (see section 3.2). Additionally, we compared our data with the predictions of the model proposed by Sato (2005). In both cases the viscosity of andesitic melts computed after Vetere et al., (2008) was used in the calculation assuming a Fe^{2+}/Fe_{tot} ratio of 0.7 for the melt. This ratio was experimentally determined in andesitic melts at similar conditions as used in our study (Vetere et al., 2008). At more oxidizing conditions (e.g., $Fe^{2+}/Fe_{tot} = 0.4$) the melt viscosity would be slightly higher by about 0.3 log units.

Our falling sphere data indicate a much larger effect of dispersed crystals on melt viscosity than predicted by the Einstein-Roscoe equation while the agreement with the model of Sato (2005) is much better (Fig. 6).

When we fit the equation of Einstein-Roscoe to the present experimental data, we obtain a constant ω of about 0.3, indicating that the crystal mush may become rigid at a crystallinity of ~ 30 vol%. This is similar to the critical rigidity threshold of a crystal mush determined in basaltic samples by Philpotts and Carroll (1996) and Hoover et al. (2001), who showed that heating of a basalt cube caused collapse of the cube only after melting 65-80% of the basalt (crystallinity of 0.20-0.35).

At 1523 K the experimental data are coincident with the predictions of Sato (2005). At 1473 K the measured effective viscosity of the crystal-melt suspension with a melt water content of ~ 4 wt% is about 0.1 log units higher than the predictions after the equation of Sato (2005). The only significant deviation from the model of Sato (2005) is observed for the low temperature data at 1373 K (deviation of 0.8 log units), but as emphasized above, the relative viscosity η_r at 1373 K is higher than η_r determined at higher temperatures. Thus, the viscosity value at 1373 K has to be interpreted with caution.

Considering that both the dataset of Sato (2005) and the dataset produced in this study yielded viscosities which are higher than those predicted using the Einstein-Roscoe model with the parameters proposed by Marsh (1981), we conclude that the application of this model will lead to a minimum estimation of the effective viscosity. The difference between the experimental values and the theoretical values may be explained by the assumption of spherical particles (circular in 2D) in the Einstein-Roscoe model, ignoring also surface roughness (assuming FF = 1). On the other hand, the model of Sato (2005) has been developed on the basis of viscosity experiments with non-spherical, rough crystals. As mentioned above the zircon crystals used in our study have irregular shape (FF=0.5-0.6; Fig. 5). Thus, the roughness of crystals may be an important parameter influencing the rheological properties of crystal mushes.

For the experiments performed with high crystals contents (30-40 vol%) at 1523 K we can estimate only a minimum effective viscosity. However, a minimum yield strength (a value higher than 130 Pa) is obtained. At run durations up to 16 hours (Zr40 and Zr13B, Table 3) the settling distance was less than 0.1 mm. Hence, the effective viscosity is estimated to be $>10^6$ Pa s for these experiments, i.e., more than 100 times higher than estimated by literature models (more than two order of magnitude higher than that estimated by literature models (Costa, 2005, and references therein). The experiments indicate that the transition from melt-like behavior to solid-like behavior of a magma may occur at significantly lower crystal fraction than the commonly assumed values of 0.4-0.6 (e.g., Lejeune and Richet, 1995; March, 1981). It appears that in particular the aspect ratio and the form factor play a very important role.

Limitations of the falling sphere technique for effective viscosity determinations: Newtonian versus non Newtonian behavio*r*

Our observations indicating that the rheological properties of mushes are strongly changing between 15-30 vol% of crystals are consistent with previous datasets from Arbaret et al. (2007) and Sato (2005). Although the viscosities in the experiments of Arbaret et al. (2007) were much higher (10^9-$10^{12.5}$ Pa·s) than in our experiments (granitic melts), a Newtonian behavior was only observed for crystal volumes between 0 and 16 vol%. As a consequence the effective viscosity increases strongly with crystal fraction between 16 and 54 vol%, i.e., by more than one order of magnitude at a fixed strain rate of $6 \cdot 10^{-4}$ s^{-1}.

A noticeable deviation from Newtonian behavior was already observed at 1443 K by Sato (2005) in a basalt

system containing 11 vol% of plagioclase and the effect becomes more pronounced at lower temperatures, i.e., at higher crystal fractions. The decrease in apparent viscosity with increasing shear rate was attributed to the alignment of plagioclases parallel to the tangential direction of the rotation of the rod in the rotational viscometer experiments. The decrease of the viscosity of the suspension caused by time-dependent alignment of non-spherical particles was observed also in other studies to (e.g., Deubener and Brückner, 1997; Pinkerton and Norton, 1995). Hoover et al. (2001) demonstrated that the yield strength (e.g., the stress at which a material begins to deform plastically) occurs at much lower crystals fraction (0.1–0.2) for prismatic kaolin suspensions compared to spherical poppy seed suspensions (about 0.5).

Alignment of crystals was not operative in our experiments both because of the small aspect ratios of the crystals and because of the applied experimental technique. The sphere penetrates always into a melt with chaotic arrangement of crystals (see Fig. 1). No change in morphology of the crystal – melt system was observed in the sample after the movement of the sphere (especially behind the sphere). The situation may be different in case of more elongated crystals such as plagioclase. However, this was not tested in our study. The strong increase in effective viscosity between 15 vol% and 30 vol% in our experiments is probably due to the roughness of crystals characterized by the FF parameter and to the formation of a connected network of crystals between 15 vol% and 30 vol% (the parameter FF influences the point at which crystals form a connected network). Clearly in our experiments the force imposed by the Pt sphere was not large enough to break the network of crystals, at least in samples containing 30 vol% of crystals.

Implications for magma ascent in dikes

Our results have profound implication on the calculation of the ascent velocity of magmas. Lister and Kerr (1991) proposed the following relation to estimate the uprising velocity u of magma in a dike of width w:

$$u = (w^2/3\eta)\Delta\rho g \qquad (7),$$

where $\Delta\rho$ is the difference between the density of country rock and that of the magma ($\Delta\rho = 250$ kg/m^3) and g is the gravity (9.81 m/s^2). Selecting w between 1 and 10 m, and using the effective viscosities from our experimental data and from literature models depicted in Figure 8, we computed u with Eq. (7) for andesitic magmas with 0.5 wt% dissolved H_2O (in the melt) at 1523 K. Results are reported in Figure 8.
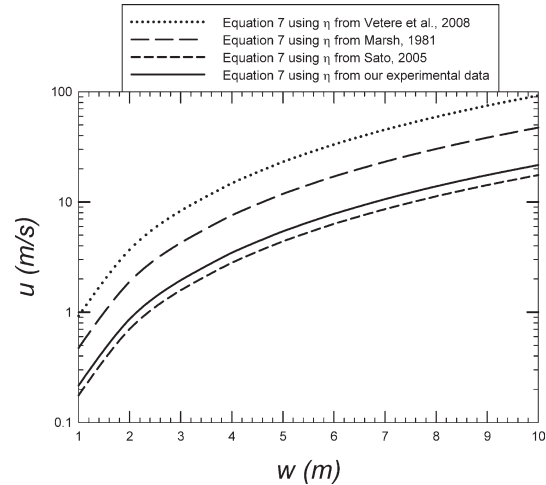

Figure 8. Variation of the ascent velocity u as function of width (w) of a dike for an andesitic magmas with 15 vol% crystal (T = 1523 K; 0.50 wt % H_2O). The curves represent velocity calculations using Eq. (7) based on the effective viscosity from our experimental data (solid line), the model of Sato (2005) (short dashed line) and from the Einstein-Roscoe Equation using the parameters proposed Marsh (1981) (long dashed line) and melt viscosity after Vetere et al., (2008) (dotted line).

There are no significant differences between the calculated velocities using our experimental data and those derived with the Sato (2005) model (Fig. 8). Velocities based on the viscosity calculated by the Einstein-Roscoe equation using the parameter of Marsh (1981) are higher by a factor of 2. The velocity of pure andesitic melts is nearly one log unit higher than that of a andesitic mush containing ~ 15 vol% crystals. However, it has to be emphasized that Eq. (7) is a rough estimate of flow velocity because it does not consider the possible shear-rate dependence of viscosity, the time-dependent effects such as the alignment of crystals, and the real structure of the dykes, which may be characterized by abrupt changes in thickness. Thus a transfer of experimental data (or viscosity models) to nature has always to be treated with caution.

CONCLUDING REMARKS

Falling sphere is an appropriate method to investigate rheological properties of partially crystallized magmatic systems at low crystal content, i.e., dilute dispersions. Adjusting defined crystal fraction of magmas via addition of zircons has the big advantage to vary the crystal content independent from melt composition. This enables as well the variation of temperature over a wide range without significant changes in the system, i.e. inference of superimposed crystallization processes is avoided. Thus, falling sphere experiments performed on melts doped with zircon

crystals is a well suited method to investigate systematically magma rheology at conditions relevant to nature. The limitation, however, is given by the shear force imposed by the sphere which is insufficient to initiate movement of the sphere at high crystal fraction (»15 vol%).

ACKNOWLEDGMENTS

REFERENCES

Arbaret, L., Bystrycky, M. and Champallier, R. (2007) Microstructures and rheology of hydrous synthetic magmatic suspensions deformed in torsion at high pressure. Journal of Geophysical Research, 112, B10208.

Behrens, H. (1995) Determination of water solubilities in high-viscosity melts: An experimental study on $NaAlSi_3O_8$ and $KAlSi_3O_8$ melts. European Journal of Mineralogy, 7, 905-920.

Behrens, H. and Schulze, F. (2003) Pressure dependence of melt viscosity in the system $NaAlSi_3O_8$-$CaMgSi_2O_6$. American Mineralogist, 88, 1351-1363.

Berndt, J., Liebske, C., Holtz, F., Freise, M., Nowak, M., Ziegenbein, D., Hurkuck, W. and Koepke, J. (2002) A combined rapid-quench and H_2-membrane setup for internally heated pressure vessels: description and application for water solubility in basaltic melts. American Mineralogist, 87, 1717-1726.

Botcharnikov, R.E, Holtz, F., Almeev, R.R., Sato, H. and Behrens H. (2008) Storage conditions and evolution of andesitic magma prior to the 1991-95 eruption of Unzen volcano: Constraints from natural samples and phase equilibria experiments. Journal of Volcanology and Geothermal Research, 175, 168-180.

Boudreau, A.E. (1999) PELE: a version of the MELTS software 70 program for the PC platform. Computational Geosciences, 25, 201-203.

Caricchi, L., Burlini, L., Ulmer P., Gerya, T., Vassalli, M. and Papale, P. (2007) Non-Newtonian rheology of crystal-bearing magmas and implications for magma ascent dynamics. Earth and Planetary Science Letters, 264, 402-419

Champallier, R., Bystrichy, M. and Arbaret, L. (2008) Experimental investigation of magma rheology at 300 MPa: From pure hydrous melt to 76 vol.% of crystals. Earth and Planetary Science Letters, 263, 571-583.

Chen, H.C., De Paolo, D.J., Nakada, S. and Shieh, Y.M. (1993) Relationship between eruption volume and neodymic isotopic composition at Unzen volcano. Nature, 362, 831-834.

Costa, A. (2005) Viscosity of high crystal content melts: Dependence on solid reaction. Geophysical Research Letters, 32,

L22308.

Cox, M.R. and Budhu, B. (2008) A practical approach to grain shape quantification. Engineering Geology, 96, 1-16.

Deer, W.A., Howie, R.A. and Zussman, J. (1992) An Introduction to the Rock-Forming Minerals (2nd edition). pp. 696, Longman, Harlow.

Dellino, P. and La Volpe, L. (1996) Image processing analysis in reconstructing fragmentation and transportation mechanisms of pyroclastic deposits. The case of Monte Pilato-Rocche Rosse eruptions, Lipari (Aeolian islands, Italy). Journal of Volcanology and Geothermal Research, 71, 13-29.

Deubener, J. and Brückner, R. (1997) Influence of nucleation and crystallization on the rheological properties of lithium disilicate melt. Journal of Non-Crystalline Solids, 209, 96-111.

Einstein, A. (1906) Eine neue Bestimmung der Molekuldimensionen. Annals of Physics, 19, 289-306.

Faxen, H. (1923) Die Bewegung einer starren Kugel längs der Achse eines mit zäher Flüssigkeit gefüllten Rohres. Arkiv för Matemetik Astronomi och Fysik, 17, 1-28 (in German).

Getson, J.M. and Whittington, A.G. (2007) Liquid and magma viscosity in the anorthite-forsterite-diopside-quartz system and implications for the viscosity-temperature paths of cooling magmas. Journal of Geophysical Research, 112, B10203.

Giordano, D., Russel, K.J.and Dingwell, D.B. (2008) Viscosity of magmatic liquids: a model. Earth and Planetary Science Letters, 271, 123-134.

Harris, A.J.L. and Rowland, S.K. (2001) FLOWGO: A kinematic thermo-rheological model for lava flowing in a channel. Bulletin of Volcanology, 63, 20-44.

Hui, H. and Zhang, Y. (2007) Toward a general viscosity equation for natural anhydrous and hydrous silicate melts. Geochimica et Cosmochimica Acta, 71, 403-416.

Hoover, S.R., Cashman, K.V., Manga, M. (2001) The yield strength of subliquidus basalts - experimental results. Journal of Volcanology and Geothermal Research, 107, 1-18.

Iezzi, G. and Ventura, G. (2002) Crystal fabric evolution in lava flows: results from numerical simulations. Earth and Planetary Science Letters, 200, 33-46.

Ishibashi, H. (2009) Non-Newtonian behavior of plagioclase-bearing basaltic magma; Subliquidus viscosity measurements of the 1707 basalt of Fuji volcano. Japan. Journal of Volcanology and Geothermal Research, 181, 78-88.

Kahle, A., Winkler, B.and Hennion, B. (2003). Is Faxén's correction function applicable to viscosity measurements of silicate melts with the falling sphere methods? Journal of Non-Newtonian Fluid Mechanics, 112, 203-215.

Kerr, R.C. and Lister, J.R. (1991) The effects of shape on crystal settling and on the rheology of magmas. Geology, 99, 457-467.

Lejeune, A.M. and Richet, P. (1995) Rheology of crystal-bearing silicate melts - an experimental study at high viscosities. Journal of Geophysical Research, 100, 4215-4229.

Leschik, M., Heide, G., Frischat, G., Behrens, H., Wiedenbeck, M., Wagner, N., Heide, K., Geißler, H. and Reinholz, U. (2004) Determination of H_2O and D_2O contents in rhyolitic glasses using KFT, NRA, EGA, IR spectroscopy, and SIMS. Physics and Chemistry of Glasses, 45, 238-251.

Lister, J.R. and Kerr, R.C. (1991) Fluid-Mechanical models of crack propagation and their application to magma transport in dyke. Journal of Geophysical Research, 96, 10049-10077.

Loncaric, S. (1998) A survey of shape analysis techniques. Pattern Recognition, 31, 983-1001.

Mandal, N., Chakraborty, C.and Samanta, S.K., (2000) An analysis of anisotropy of rocks containing shape fabrics of rigid inclusions. Journal of Structural Geology, 22, 831-839.

Marsh, B.D. (1981) On the crystallinity, probably occurrence, and rheology of lava and magma. Contributions to Mineralogy and Petrology, 78, 85-98.

Misiti, V., Freda, C., Taddeucci, J., Romano, C., Scarlato, P., Longo, A., Papale, P. and Poe, B.T., (2006). The effect of H_2O on the viscosity of K-trachytic melts at magmatic temperatures. Chemical Geology, 235, 124-137.

Philpotts, A.R. and Carroll, M., (1996) Physical properties of partly melted tholeiitic basalt. Geology, 24, 1029-1032.

Pinkerton, H. and Norton, G. (1995) Rheological properties of basaltic lavas at sub-liquidus temperatures: laboratory and field measurements on lavas from Mount Etna. Journal of Volcanology and Geothermal Research, 68, 307-323.

Pinkerton, H. and Stevenson R.J. (1992) Methods of determining the rheological properties of magmas at suliquidus temperature. Journal of Volcanology and Geothermal Research, 53, 47-66.

Roscoe, R. (1952) The viscosity of suspensions of rigid spheres. British Journal of Applied Physics, 3, 267-269.

Rosenberg, C.L. and Handy, M.R. (2005) Experimental deformation of partially melted granite revisited: Implication for the continental crust. Journal of Metamorphic Geology, 23, 19-28.

Russell, J.K., Girdano, D., Dingwell, D.B. (2003) High-temperature limits on viscosity of non-Arrhenian silicate melts. American Mineralogist, 88, 1390-1394.

Sato, H. (2005) Viscosity measurements of subliquidus magmas: 1707 basalt of Fuji volcano. Journal of Mineralogical and Petrological Sciences, 100, 133-142.

Scarfe, C.M., Mysen, B.O. and Virgo, D. (1987) Pressure dependence of the viscosity of silicate melts. In Magmatic processes: physicochemical principles (Mysen, B.O. Ed.). The Geochemical Society (University Park, Pensylvania), Special publication, 1, 59-67.

Shaw, H.R. (1963) Obsidian-H_2O viscosities at 100 and 200 bars in temperature range 700 degrees to 900 degrees C. Journal of Geophysical Research, 68, 6337-6343.

Shaw, H.R. (1972) Viscosities of magmatic silicate liquids - Empirical method of prediction. American Journal Science, 272, 870-893.

Sherman, P. (1968) Emulsion science. pp. 351, Academic Press, London, New York.

Simha, R. (1940) The influence of Brownian movement on the viscosity of solutions. The Journal of Physical Chemistry, 44, 25-34.

Vetere, F. (2006) Viscous flow of magmas from Unzen volcano, Japan - implication for magma mixing and ascent. pp. 162, Ph.D. thesis, University of Hannover, Hannover, Germany.

Vetere, F., Behrens, H., Holtz, F. and Neuville, D.(2006) Viscosity of andesitic melts — new experimental data and a revised calculation model. Chemical Geology, 228, 233-245.

Vetere, F., Behrens, H., Schuessler, J.A., Holtz, F., Misiti, V.,and Borchers, L. (2008) Viscosity of andesite melts and its implication for magma mixing prior to Unzen 1991-1995 eruption. Journal of Volcanology and Geothermal Research, 175, 208-217.

Watson, E.B. and Harrison, T.M. (1983) Zircon saturation revisited: temperature and composition effect in variety of crustal magma types. Earth and Planetary Science Letters, 64, 295-304.